# Probing the polarity of ferroelectric thin films with x-ray standing waves

M. J. Bedzyk

*Department of Materials Science and Engineering and Materials Research Center, Northwestern University, Evanston, Illinois 60208*
*and Materials Science Division, Argonne National Laboratory, Argonne, Illinois 60439*

A. Kazimirov

*Department of Materials Science and Engineering and Materials Research Center, Northwestern University, Evanston, Illinois 60208*

D. L. Marasco

*Department of Materials Science and Engineering and Materials Research Center, Northwestern University, Evanston, Illinois 60208*
*and Materials Science Division, Argonne National Laboratory, Argonne, Illinois 60439*

T.-L. Lee

*Department of Materials Science and Engineering and Materials Research Center, Northwestern University, Evanston, Illinois 60208*

C. M. Foster

*Materials Science Division, Argonne National Laboratory, Argonne, Illinois 60439*
*and Advanced Micro Devices, 5204 East Ben White Boulevard, Austin, Texas 78741*

G.-R. Bai

*Materials Science Division, Argonne National Laboratory, Argonne, Illinois 60439*

P. F. Lyman and D. T. Keane

*Department of Materials Science and Engineering and Materials Research Center, Northwestern University, Evanston, Illinois 60208*
(Received 26 October 1999)

An x-ray-diffraction method that directly senses the phase of the structure factor is demonstrated and used for determining the local polarity of thin ferroelectric films. This method is based on the excitation of an x-ray standing-wave field inside the film as a result of the interference between the strong incident x-ray wave and the weak kinematically Bragg-diffracted x-ray wave from the film. The method is used to sense the displacements of the Pb and Ti sublattices in single-crystal $c$-domain $PbTiO_3$ thin films grown by metal-organic chemical-vapor deposition on $SrTiO_3(001)$ substrates.

Ferroelectricity in solids originates from relative shifts of the anion and cation atomic sublattices,[1] resulting in a net dipole moment (spontaneous polarization) along a certain crystallographic axis. Under an applied electric field, the direction of the polarization vector can be switched. This bistable property can provide the basis for nonvolatile random access memory. Figure 1 depicts the polarized ''up'' and ''down'' unit cells for the ferroelectric $PbTiO_3$ perovskite structure with opposite dipole moments along the [001] polar axis due to the displacements of the $Pb^{2+}$ and $Ti^{4+}$ sublattices with respect to the $O^{2-}$ sublattice. In bulk ferroelectric crystals it is widely accepted that the lattice polarization and its evolution under an external electric field cannot be studied by conventional x-ray-diffraction techniques, since diffraction introduces a center of symmetry by Friedel's law and therefore cannot distinguish up from down in Fig. 1. Also, the dipole moments of the unit cells are perfectly aligned only within single-domain volumes with typical sizes smaller than the $10-100-\mu m$ x-ray-absorption length. Recently, single-crystal ferroelectric thin films with thicknesses much less than the typical domain size in bulk crystals have been grown using various synthesis methods.[2] The ability to control the domain structure, together with a

technique to precisely characterize the sublattice displacements and polarization state, would be a powerful combined approach for investigating such fundamental phenomena in ferroelectricity as polarization switching and switching-induced polarization degradation (i.e., fatigue).

Standard x-ray-diffraction methods have been successfully applied to study the growth of $c$ and $a$ domains in ferroelectric thin films. These measurements are based on the separation in reciprocal space of the x-ray-diffraction peaks of the $a$ and $c$ domains. For metal-organic chemical-vapor deposition (MOCVD) grown $PbTiO_3$ films on $SrTiO_3(001)$ substrates, the formation of $a$ domains can be totally suppressed below a critical thickness of 500–700 Å, and coherently strained single-crystal $c$-domain films are grown.[3] A remaining question is whether these $c$ domains are polarized up or down. The crystal truncation rod (CTR) method, based on the interference between the waves scattered from the substrate and the film,[4] was used recently to measure the offset between the lattices of the film and substrate, and the polarization direction of a 100-Å $PbTiO_3$ film.[5] In the present paper we report a phase-sensitive approach that uses the x-ray standing wave (XSW) generated inside the thin epitaxial film during Bragg diffraction from the film to determine the polarity of the film.
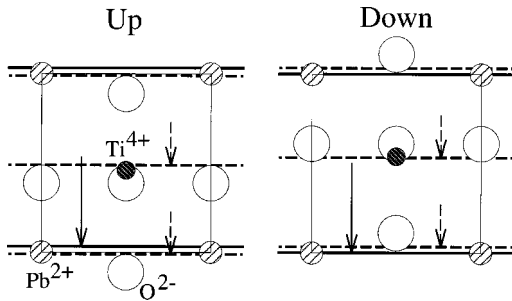
FIG. 1. The *a* axis projection of the PbTiO$_3$ tetragonal ''up'' and ''down'' perovskite unit cells. For the bulk unit cell at 20 °C $a=3.905$ Å and $c=4.156$ Å. For the up unit cell with the origin chosen to coincide with the Pb$^{2+}$ ion, the fractional *c*-axis displacement of the three O$^{2-}$ ions from the face-centered positions is $-0.112$ and the Ti$^{4+}$ ion from the body-centered position is $-0.040$ (Ref. 1). In comparison, SrTiO$_3$ is a cubic perovskite with $a=3.905$ Å at 20 °C (Ref. 1). The solid and dashed horizontal lines mark the lattice positions of the (001) and (002) diffraction planes, respectively. The solid and dashed arrows mark the inward path from start to finish that the XSW antinode follows as angle $\theta$ is advanced through the (001) and (002) reflections, respectively.

The XSW method is based on generating a standing wave inside a crystal from the interference between the incident and Bragg-diffracted x-ray plane waves.[6] Such a standing wave has the periodicity of the diffraction planes $d_{hkl}$, and can be phase shifted inward by $d_{hkl}/2$ by scanning the incident angle through the Bragg peak. This phase shift of the XSW can be observed by monitoring the characteristic fluorescence from atoms within the crystal.[6] The standard XSW method is applied to perfect crystals that exhibit Bragg reflection widths measured in arc seconds. Within this ''Bragg band gap'' the *E*-field amplitude of the diffracted plane wave $E_H$ approaches that of the incident wave $E_0$ (i.e., the reflectivity $R=|E_H/E_0|^2\approx1$). Thus the XSW field at or near the surface has a strong spatial contrast with the visibility [$V=(I_{max}-I_{min})/(I_{max}+I_{min})$] of the interference fringes approaching unity. For a compound crystal the measurement of the fluorescence yield from the atoms of the *j*th sublattice excited by the x-ray standing wave can be used for directly determining of the phase of the structure factor.[7] Neglecting the extinction effect the fluorescence yield from the *j*th sublattice can be written as[8]

$$Y_H^j(\theta) = 1 + R(\theta) + 2\sqrt{R(\theta)}|S_H^j|e^{-M_H^j-W_H^j}\cos[\nu(\theta)-\varphi_H^j],$$

where $|S_H^j|$ and $\varphi_H^j$ are the modulus and the phase of the geometrical structural factor of the *j*th sublattice: $S_H^j=|S_H^j|\exp(i\varphi_H^j)=\Sigma\exp(2\pi i\vec{H}\cdot\vec{r}_n^j)$; $\exp(-M_H^j)$ and $\exp(-W_H^j)$ are the thermal and static Debye-Waller factors, respectively; and $\nu(\theta)$ is the phase of the complex *E*-field amplitude ratio $E_H/E_o$. Thus the phase and the modulus of the geometrical structure factor of the *j*th sublattice can be extracted directly from the interference term, making the XSW method phase sensitive. Since the phases of the Pb and Ti sublattice structure factors are different for the up and down unit cells, there will be different angular dependencies for the fluorescence yields from these two oppositely polarized structures.

The standard XSW method, that uses dynamical Bragg diffraction from a bulk perfect crystal for generating the XSW, has been successfully applied to surface structure determination for the past two decades.[9] More recently it was shown[10,11] that thin-film Bragg diffraction is also accompanied by an XSW field. Since this XSW is generated inside a thin film with a thickness much less than the extinction length, kinematical diffraction theory can be used for calculating the *E* fields with reasonable accuracy. The XSW field originates from the interference between the incident x-ray wave and the very weak wave scattered from the thin film, resulting in a very weak visibility of the interference fringes of $V\approx2\sqrt{R}$ at (or near) the top surface of the film. This will range from 0.01 to 0.1 depending on the film thickness. Deeper into the film *V* decreases due to the decrease in $E_H(z)$, with $E_H=V=0$ at the bottom of the film. Measuring such a small modulation in the fluorescence yield from an atom within the film typically requires the accumulation of $10^6$ fluorescence counts from that atomic species at each angular step of the rocking curve scan. The high x-ray intensity from an insertion device at a third-generation synchrotron source makes this requirement more readily achievable.

As a first demonstration of using the thin-film XSW method to determine the local polarity of a ferroelectric film, we studied three PbTiO$_3$ thin-film samples grown by MOCVD on SrTiO$_3$(001) substrates. The film thicknesses were 100, 200, and 400 Å. (See Ref. 12 for a detailed discussion of the sample preparation.) We used the 5ID-C and 12ID-D undulator stations at the Advanced Photon Source with Si(111) *L*-N$_2$ cooled double-crystal monochromators. The $5\times5$-mm$^2\times1$-mm-thick samples were mounted on a four circle diffractometer for scattering in the vertical plane. The x-ray fluorescence from the sample was monitored with an energy-dispersive solid-state detector. Both the fluorescence and scattered x-ray reflected intensity were recorded as functions of incident angle $\theta$. The incident beam slit was typically 0.4 mm wide by 0.2 mm high. Several different lateral positions on each sample were examined. The analysis of the rocking curves (Fig. 2) with their pronounced thickness oscillations attests to the high crystalline quality of the films and abruptness of the substrate-film interface. The Pb-*L* experimental data measured at an incident energy of 13.50 keV for the 400-Å-thick film are shown in Figs. 2(a) and 2(b) for the (001) and (002) Bragg reflections, respectively. As can be seen, the Pb-*L* peak-to-peak modulation approaches $2\sqrt{R}$, as predicted from the fringe visibility discussion.

While the experimental XSW results from the Pb sublattice are sufficient for the analysis of the film polarity, the measurement of the fluorescence yield from a second (Ti) sublattice can be used as a stringent test for the consistency of the structural model depicted in Fig. 1. Specifically, the measurement should be very sensitive to the model prediction that the Ti layer in the down polarized film is 0.33 Å further above the Pb layer than it is in the up polarized film. For the Ti XSW measurement, it was necessary to collect the Ti *K* fluorescence from within the film while completely suppressing the collection of the Ti *K* fluorescence from the underlying SrTiO$_3$ substrate. This was accomplished by using the evanescent-wave emission technique,[13,14] that measures the fluorescent signal at small take-off angles. (The
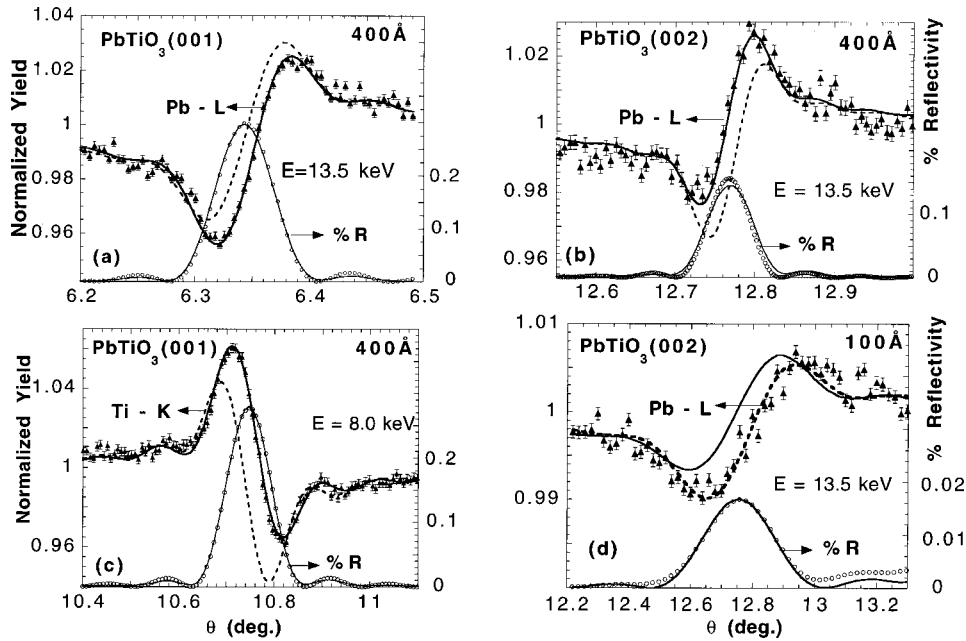
FIG. 2. The experimental XSW data measured from a [(a)–(c)] 400-Å-thick and (d) 100-Å-thick PbTiO$_3$ film. (a) The angle $\theta$ dependence of the normalized Pb-$L$ fluorescence yield and reflectivity in the vicinity of the PbTiO$_3$(001) reflection at an incident energy of 13.5 keV. [(b) and (d)] The Pb-$L$ fluorescence yield and (002) reflection at 13.5 keV. (c) The Ti-$K\alpha$ fluorescence yield and (001) reflection measured at 8.0 keV using the evanescent-emission wave emission technique. The best fits for the up and down polarities are shown as solid and dashed lines, respectively.

critical angle is 0.65° for 4.51-keV Ti-$K\alpha$ fluorescence x rays escaping from PbTiO$_3$). We used a take-off angular range of 0° to 0.6°, over which the probed depth was significantly smaller than the 400-Å thickness of the PbTiO$_3$ film. The Ti $K$ (001) XSW results for the 400-Å film that were obtained at an incident x-ray beam energy of 8.00 keV are shown in Fig. 2(c).

Perhaps the most noticeable feature in the data is the counterphase relationship between the (001) Pb and Ti modulations in Figs. 2(a) and 2(c). This observation, which is due to the approximately $d_{001}/2$ separation between the Ti and Pb atomic planes, illustrates most dramatically the fundamental phase (or structural) sensitivity of the XSW experiment. As shown earlier[7] for the case of dynamical diffraction from a semi-infinite single crystal, the XSW phase is directly linked to the phase $\beta_H$ of the structure factor $F_H = \Sigma f_H^j S_H^j$. Physically, the XSW antinodes shift inward in the $-\mathbf{H}$ direction by exactly $d_H/2$ when the incident angle $\theta$ is advanced through the $hkl$ Bragg reflection. Referring to the path marked by the arrows in Fig. 1, this inward shift starts with the XSW antinodes aligned halfway between diffraction planes on the low-angle side of the reflection, and ends with the antinodes aligned with the diffraction planes on the high-angle side. Under this definition the absolute lattice position of the $hkl$ diffraction planes are defined[7] as coinciding with the maxima that appear in the real part of the $hkl$ Fourier component of the scattering density max[Re[$\rho_H(\mathbf{r})$]], where $\rho_H(\mathbf{r}) = (1/V) F_H \exp(-2\pi i \mathbf{H} \cdot \mathbf{r})$. Based on this definition and referring to the solid horizontal lines in Fig. 1, the (001) diffraction planes are slightly displaced from the Pb planes by a fractional $c$-axis displacement of $\beta_{001}/2\pi = 0.063$ for the up unit cell, and by $-0.001$ for the down unit cell.[15] The above derivation[7] and arguments serve to establish a physical origin for the XSW within the crystal lattice. This lattice (Fig. 1) will then be used as a model for a consistency test against the XSW data (Fig. 2). The arrows in Fig. 1 mark the inward path that the antinodes follow for a $\theta$ scan through the reflection. For the polarized up unit cell, scanning through the (001) peak causes the antinode to pass through

the center of the Ti-atom layer, but not the Pb center whereas the opposite is true for the down unit cell. This is the basis for the phase differences in the modulations for the up and down yield curves shown in Fig. 2. It is also the basis for the polarity-sensing capability of this measurement.

Another interesting observation is that the amplitude of the XSW induced modulation of the Ti-$K$ fluorescence yield is nearly twice that of the Pb-$L$ yield, [see Figs. 2(a) and 2(c)]. This is due to the fact that the evanescent-wave technique applied to the Ti signal makes it more surface sensitive, and that the visibility of the interference fringes is highest at the top of the film. This combination of the XSW and evanescent-wave techniques is used to test the uniformity of polarity as a function of depth into the film.

Even though kinematical theory can be used in a reasonable approximation to analyze the experimental data, we developed[16] a more rigorous computational algorithm based on Takagi-Taupin[17] dynamical diffraction theory for calculating the total $E$-field intensity inside of a single crystal heteroepitaxial thin-film structure. As a first approximation, we assumed that the film had a single, either up or down polarity, as depicted and parametrized in Fig. 1. The 400-Å experimental yield curves were fitted for up and down unit cells using the static Debye-Waller factor as the only fitting parameter. The fits shown in Figs. 2(a)–2(c) unambiguously reveal that the 400-Å film is polarized up. Furthermore, the combined Pb and Ti results allow us to conclude that, to within the 1% $\Delta d/d$ accuracy of the XSW analysis, the fractional $c$-axis displacements of both the Pb$^{2+}$ and Ti$^{4+}$ sublattices in the film are in agreement with the bulk-like values listed in Fig. 1. As a second-order approximation, we allowed for the coexistence of polarized up and down domains. However, this did not lead to an improvement in $\chi^2$ or to any significant fraction of coexisting down domains.

For other lateral positions on this 400-Å-thick film, we found variances in the static Debye-Waller factor ranging from 0.7 to 0.9, but all domains were found to be polarized up. Interestingly, when we examined various lateral positions on 100- and 200-Å-thick films, we found domains polarized

down and other domains polarized up. The Pb $L$ (002) data and analysis for a down domain of the 100-Å-thick film is shown in Fig. 2(d). The XSW analysis of this particular domain agreed with the earlier CTR measurement reported for this same 100-Å PbTiO$_3$/SrTiO$_3$(001) sample.[5]

Our finding for the 400-Å film of a single polarization state in an as-grown ferroelectric film is intriguing. Since the PbTiO$_3$ film is grown at a temperature of 700–750 °C, much higher than the transition temperature reported for the bulk PbTiO$_3$ (490 °C),[1] one expects that the transition from the paraelectric to ferroelectric phase occurs during the cooldown process. One may also expect a random nucleation of up and down domains on an ideally terminated nonpolar SrTiO$_3$(001) surface. Our observed preferential polarization for the 400-Å film may be a thickness effect, or it may indicate a more uniform structural modification in the topmost atomic layers for that particular substrate at the transition temperature. For our measurements as-polished commercial SrTiO$_3$(001) substrates were used for the growth. These are known to have both Ti- and Sr- terminated surface regions with 75–98 % being TiO$_2$ terminated.[18] Methods for preparing well-ordered SrTiO$_3$(001) surfaces were recently reported[18,19] that produce atomically flat uniform Ti-terminated surfaces. The application of thin-film XSW technique to study ferroelectric films grown on atomically controlled surfaces should provide information about the relationships between termination, relaxation of the SrTiO$_3$ surface, and polarization of the grown film. In addition, fully epitaxial ferroelectric capacitor structures have recently been grown.[20] Real-time XSW techniques could be applied to these structures while being poled (or switched) by external electric fields. This approach could effectively be used to study the dynamics of switching and degradation processes in modeled ferroelectric capacitor devices.

In addition to structural studies of thin films, one can also use this thin-film version of the XSW technique to study adsorbate surface structures on single-crystal epitaxial films that cannot be grown as bulk single crystals. This will open up the application of XSW analysis to a much larger array of surface structures.

[1] F. Jona and G. Shirane, *Ferroelectric Crystals* (Dover, New York, 1993), and references therein.

[2] See, e.g., *Ferroelectric Thin Films: Synthesis and Basic Properties*, edited by C. A. Paz de Araujo, J. F. Scott, and G. W. Taylor (Gordon and Breach, New York, 1996).

[3] C. M. Foster *et al.*, J. Appl. Phys. **78**, 2607 (1995).

[4] I. K. Robinson, R. T. Tung, and R. Feidenhans'l, Phys. Rev. B **38**, 3632 (1988).

[5] C. Thompson *et al.*, Appl. Phys. Lett. **71**, 3516 (1997).

[6] B. W. Batterman, Phys. Rev. Lett. **22**, 703 (1969).

[7] M. J. Bedzyk and G. Materlik, Phys. Rev. B **32**, 6456 (1985).

[8] A. Kazimirov, M. Kovalchuk, and V. Kohn, Pis'ma Zh. Tekh. Fiz. **14**, 1345 (1988) [Sov. Tech. Phys. Lett. **14**, 587 (1988).]

[9] P. L. Cowan, J. A. Golovchenko, and M. F. Robbins, Phys. Rev. Lett. **44**, 1680 (1980).

[10] A. Kazimirov *et al.*, Solid State Commun. **104**, 347 (1997).

[11] A. Kazimirov *et al.*, J. Appl. Phys. **84**, 1703 (1998).

[12] C. M. Foster *et al.*, J. Appl. Phys. **79**, 1405 (1996).

[13] S. Becker, J. A. Golovchenko, and J. R. Patel, Phys. Rev. Lett. **50**, 153 (1983).

[14] T.-L. Lee *et al.*, Physica B **221**, 437 (1996).

[15] These values for the phases of the structure factor $\beta_{\pm(001)}$ were calculated at 13.50 keV, with Pb at the origin. Note that the anomalous dispersion correction factors $\Delta f'$ and $\Delta f''$ that are included in the atomic scattering factor $f_H$ cause $\beta_{hkl}$ to be energy dependent. Anomalous dispersion also causes $\beta_{001}$ to be inequivalent to $-\beta_{-(001)}$ for this case.

[16] T. L. Lee and M. J. Bedzyk (unpublished).

[17] S. Takagi, Acta Crystallogr. **15**, 1311 (1962); D. Taupin, Bull. Soc. Fr. Mineral Crystallogr. **87**, 469 (1964).

[18] M. Kawasaki *et al.*, Appl. Surf. Sci. **107**, 102 (1996).

[19] Q. Jiang and J. Zegenhagen, Surf. Sci. Lett. **367**, L42 (1996).

[20] See, e.g., C. M. Foster *et al.*, J. Appl. Phys. **81**, 3249 (1997).